Effect of electric fields on the director field and shape of nematic tactoids

Effect of electric fields on the director field and shape of nematic tactoids

Mohammadamin Safdari,[1] Roya Zandi,[1] and Paul van der Schoot[2]
[1]*Department of Physics, University of California, Riverside, California 92521, USA*
[2]*Department of Applied Physics, Eindhoven University of Technology, P.O. Box 513, 5600 MB Eindhoven, The Netherlands*

(Received 7 January 2021; accepted 6 April 2021; published 9 June 2021)

Tactoids are spindle-shaped droplets of a uniaxial nematic phase suspended in the coexisting isotropic phase. They are found in dispersions of a wide variety of elongated colloidal particles, including actin, fd virus, carbon nanotubes, vanadium peroxide, and chitin nanocrystals. Recent experiments on tactoids of chitin nanocrystals in water show that electric fields can very strongly elongate tactoids even though the dielectric properties of the coexisting isotropic and nematic phases differ only subtly. We develop a model for partially bipolar tactoids, where the degree of bipolarness of the director field is free to adjust to optimize the sum of the elastic, surface, and Coulomb energies of the system. By means of a combination of a scaling analysis and a numerical study, we investigate the elongation and director field's behavior of the tactoids as a function of their size, the strength of the electric field, the surface tension, anchoring strength, the elastic constants, and the electric susceptibility anisotropy. We find that tactoids cannot elongate significantly due to an external electric field, unless the director field is bipolar or quasibipolar and somehow frozen in the field-free configuration. Presuming that this is the case, we find reasonable agreement with experimental data.

DOI: 10.1103/PhysRevE.103.062703

I. INTRODUCTION

If an isotropic phase of rodlike colloidal particles undergoes a phase transition leading to a coexisting, uniaxially ordered nematic phase, then this typically happens via an intermediate stage characterized by an isotropic background phase in which are dispersed spindle-shaped droplets called tactoids (see Fig. 1). These tactoids eventually sediment and coalesce to form a macroscopic nematic phase, although this may take a very long time [1–6]. First discovered in 1925 by Zocher in vanadium pentoxide sols [7], who also coined the term tactoids ("Taktoide" in German), they have since been observed in a plethora of molecular, polymeric, and colloidal lyotropic liquid crystals. These include dispersions of tobacco mosaic virus particles [8], iron oxyhydroxide nanorods [9], polypeptides [10], carbon nanotubes [5,11,12], fd virus particles [13,14], F-actin fibers [15], actin filaments [16,17], chromonic liquid crystals [18], amyloid fibers [19] and cellulose nanocrystals [20–23].

The peculiar, pointy, and elongated shape of the tactoids, which reflects the underlying symmetry of the nematic phase, was initially explained in terms of the surface anchoring of the director field, presumed to be uniform [24]. The fact that the degree of elongation depends on the volume of the droplets, and that polarization microscopic images show their director field to be bipolar rather than uniform, at least if they are sufficiently large [5], reveals that this explanation is incomplete. In a bipolar configuration the director field conforms to a bi-spherical coordinate system, illustrated in Fig. 1 and in more detail in Fig. 2. If the focal points of the coordinate system reside on the poles of the droplets, representing proper surface defects known as boojums [25], the director field is then properly bipolar.

Theoretical studies of van Kaznacheev *et al.* [26,27] and Prinsen *et al.* [28–30] have revealed that the boojums are by and large virtual, situated outside of the droplet in an extrapolated director field, and that the director field is almost always incompletely bipolar and hence only quasibipolar [4,26,28,31–33]. The smaller the droplet, the further the virtual boojums move away from the poles of the droplets and the more strongly the director field resembles that of a spatially uniform director field that represents its ground state. The full crossover from uniform to bipolar director fields has only recently been observed experimentally for tactoids in dispersions of carbon nanotubes in chlorosulfonic acid, both in bulk and sessile, that is, on planar surfaces [5,12] (see Fig. 1).

What has emerged is a picture in which there are two length scales that predict the structure and shape of tactoids of a certain size. Following de Gennes, these length scales may perhaps be called extrapolation lengths, and are defined as ratios of elastic constants and surface energies [34]. These surface energies are the bare surface tension between the isotropic and nematic phases, and the surface anchoring energy penalizing a deviation from the preferred planar anchoring of the director field of elongated colloidal particles along the interface [35]. Droplets that are smaller than the smallest of these two length scales, that is, the length scale associated with the surface anchoring, tend to have a uniform director field and elongated shape. If a droplet is larger than the larger extrapolation length, which is associated with the bare surface tension, then it tends to be bipolar and nearly spherical. Droplets of a size in-between these two length

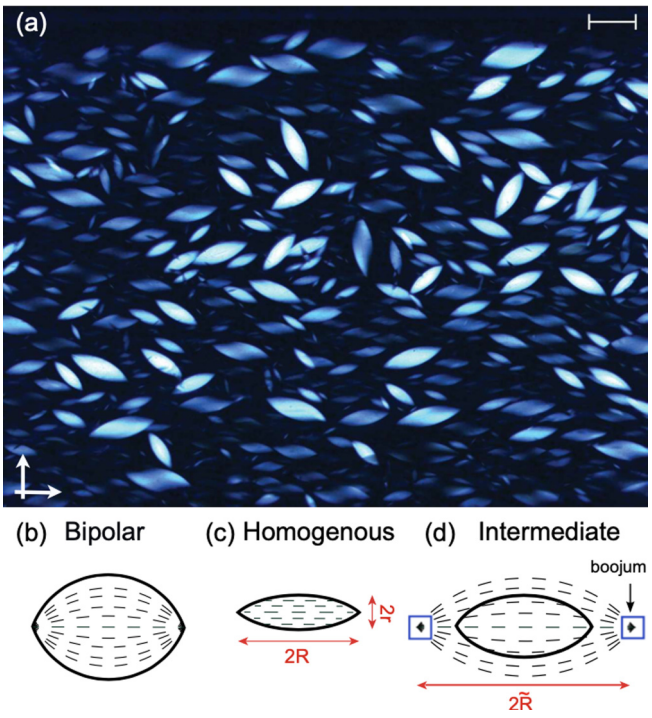

FIG. 1. (a) Polarized optical micrograph illustrating a number of nematic tactoids of different size and extinction pattern associated with the director field conformation, in a solution of carbon nanotubes in chlorosulfonic acid at 1000 ppm. Arrows show the orientation of crossed polarizers. Schematics of (b) a bipolar tactoid with boojum surface defects at the poles, (c) a homogeneous tactoid, and (d) an intermediate tactoid described by virtual boojums outside of the droplet. The parameters R and r represent the major and minor axes of the tactoid, respectively. Adopted from Ref. [5].

scales remain elongated but have director field in-between uniform and bipolar (see Fig. 1).

The situation becomes more complex if yet another length scale enters the stage. For instance, if the nematic is not uniaxial but chiral, that is, cholesteric, then the cholesteric pitch interferes with these two length scales. This gives rise to an additional regime separating uniaxial from twisted nematic (cholesteric) configurations [30,36–38]. The same is true if an

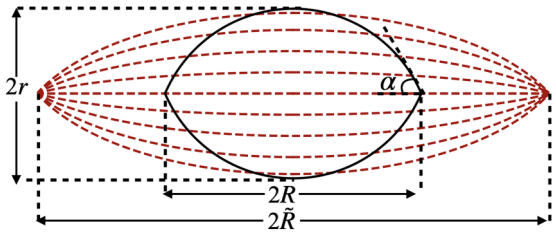

FIG. 2. Cross section (solid) and director field (dashed) of a tactoid presumed in our calculations. The droplet is cylindrically symmetric about its main axis. $2R$ denotes the length of a tactoid and $2r$ its width. $2\tilde{R}$ is the distance between the virtual boojums, which are the focal points of the (extrapolated) director field. For $R = \tilde{R}$, the virtual boojums become actual boojums, i.e., surface point defects. Also indicated is α, the opening angle of the spindle-shaped droplet (see also the main text).

external electric or magnetic field is applied to nematic rather than cholesteric tactoids. The impact of a magnetic field on tactoids of vanadium pentoxide fibers dispersed in water was investigated experimentally and theoretically by Kaznacheev *et al.*, who found that an externally applied magnetic field stretches tactoids, at least if they are sufficiently large [26]. This, indeed, points at the existence of another pertinent length scale.

The existence of such a length scale was recently confirmed by Metselaar *et al.*, who studied the impact of a high-frequency electric ac field on tactoids of chitin fibers dispersed in water [39]. These authors find very large elongations of tactoids in the presence of an electric field, with aspect ratios increasing from about 2 in zero field to about 20 for droplets larger than some critical size. Their numerical simulations, based on the lattice Boltzmann method, mimic this observation, showing that in order to obtain a very large length-to-breath or aspect ratio for the droplets, a large anchoring strength is required. Interestingly, large anchoring strengths are also known to lead to quite elongated tactoids in zero field, but the effect is apparently somehow dramatically enhanced by an electric field that arguably aligns the fibers and hence also the director field along the field direction.

If the planar anchoring of the director field to the interface between the coexisting isotropic and nematic phases were absolutely rigid and strictly bipolar, then the theory of Kaznacheev and collaborators [26] would predict an in-principle unbounded growth of the length of the tactoids with increasing electric or magnetic field strength [40]. Actually, the chitin tactoids are not actually strictly bipolar but quasibipolar, in which case the anchoring would be imperfect.

Interestingly, in the lattice Boltzmann simulations of Metselaar *et al.*, the director field seems to respond to the external alignment field not by keeping the bispherical geometry and simply stretching it, as is presumed in the calculations of Kaznacheev and coworkers. Instead, the director field seems to become uniform in the center of the droplet to bend sharply close to the interface in order to accommodate planar anchoring [41]. This is highly surprising because such a change in the geometry of the director field would require very large local deformation of the director field and associated with that would be a large elastic free energy of deformation. We should perhaps not exclude the possibility that the limited spatial resolution of the simulations produces such a strong director field deformation [41].

In this paper we delve more deeply into the problem of how external fields deform nematic tactoids, extending the theory of Kaznacheev *et al.* [26] by allowing for imperfect anchoring. By means of a combination of a scaling analysis and a numerical minimization of a free energy with a prescribed director field geometry and droplet shape, we conclude that the external field cannot produce aspect ratios that exceed those in zero field. We find a highly complex behavior characterized by no fewer than five different scaling regimes for the level of elongation and director field deformation of tactoids. If we fix the geometry of the equilibrium director field at zero field, and let only the aspect ratio respond to the external field, then we do find very large aspect ratios for large field strengths. Our predictions agree qualitatively with the experimental findings of Metselaar *et al.* [39]. This

seems to suggest that the droplet shape and the director field relax with different rates in response to an external field that is suddenly switched on. In followup work, we intend to study a two-mode relaxational dynamics model to investigate further the observations of Metselaar *et al.* [39].

The remainder of the paper is structured as follows. In Sec. II, we present our free energy that consists of a contribution of the Oseen-Frank elastic free energy, a Rapini-Papoular surface free energy, and a Coulomb free energy associated with the electric field. In Sec. III, we work out the scaling theory of fully bipolar and quasibipolar droplets in the presence of an external field, producing the various relevant length scales in the problem.

In Sec. IV, we compare the results of the variational theory that we evaluate numerically with our findings of the scaling theory, and find a very good agreement. Finally, in Sec. V we summarize our findings, compare our predictions with the experimental results of Metselaar *et al.* [39], and discuss the potential implications for our understanding of the relaxation dynamics of nematic tactoids.

II. FREE ENERGY

We consider a nematic droplet suspended in an isotropic fluid medium. The free energy F describing the droplet in an external electrical field consists of a sum of three terms

$$F = F_{\mathrm{E}} + F_{\mathrm{S}} + F_{\mathrm{C}}, \tag{1}$$

representing the Frank elastic free energy associated with a potentially deformed director field F_{E}, an interfacial free energy F_{S}, and a Coulomb energy F_{C}.

Focusing on twist-free bipolar director fields, the Frank elastic free energy of the droplet reads as [42]

$$F_{\mathrm{E}} = \int \left[\frac{1}{2} K_{11} (\vec{\nabla} \cdot \vec{n})^2 + \frac{1}{2} K_{33} (\vec{n} \times (\vec{\nabla} \times \vec{n}))^2 - \frac{1}{2} K_{24} \vec{\nabla} \cdot (\vec{n} \vec{\nabla} \cdot \vec{n} + \vec{n} \times (\vec{\nabla} \times \vec{n})) \right] dV, \tag{2}$$

where the integration is over the entire volume V of the droplet, $\vec{n}$ represents the position-dependent director field, and K_{11}, K_{33}, and K_{24} are the elastic moduli of the splay, bend, and saddle-splay deformations, respectively [34]. Here, we do not allow for twisted director fields that may arise if the bend elastic constant is sufficiently small [37]. Note that these parity-broken structures are anyway suppressed if the tactoids are elongated [30].

Within a Rapini-Papoular approximation [43], the interfacial free energy can be written as

$$F_{\mathrm{S}} = \sigma \int [(1 + \omega (\vec{q} \cdot \vec{n})^2] dA, \tag{3}$$

where σ is the interfacial tension between the nematic phase of the droplet and isotropic medium, ω is a dimensionless anchoring strength, and the integration is over the interfacial area A of the droplet. We presume that $\omega > 0$, implying that the anchoring penalizes a director field $\vec{n}$ that is not parallel to the interface, that is, at right angles to the surface normal $\vec{q}$. Rodlike particles prefer a planar anchoring of the nematic at the interface with the coexisting isotropic phase for entropy reasons [2,35,44]. In principle, both the surface tension and anchoring strength could depend on the curvature of the interface, but even for very small droplets the effect seems to be very small [33].

Finally, the Coulomb energy of a nematic droplet in an electric field $\vec{E}$ can be written as [34,45]

$$F_{\mathrm{C}} = -\frac{1}{8\pi} \epsilon_a \int (\vec{n} \cdot \vec{E})^2 dV, \tag{4}$$

where $\epsilon_a = \epsilon_{\parallel} - \epsilon_{\perp} \geqslant 0$ is the dielectric susceptibility anisotropy of the dispersion of rodlike particles, which can be described as a second-rank tensor with components $\epsilon_{\parallel}$ and $\epsilon_{\perp}$ parallel and perpendicular to the droplet axis [46]. Note that we ignore a potential permanent dipole moment on the particles and that we have not explicitly written a constant term that is not a function of the director field. It is important to note that both $\epsilon_{\parallel}$ and $\epsilon_{\perp}$ are not all that different from the dielectric constant of the isotropic phase because the dielectric response of the suspension is dominated by that of the solvent [39]. This means that any elongation of the droplets caused by an electric field is not due to a difference between the dielectric properties of the isotropic and nematic phases, as would be the case for a thermotropic nematic tactoid suspended in a polymeric fluid [47], but due to the anisotropy of the dielectric response of the nematic phase itself.

Having collected all contributions to the free energy, we need to address an issue of some contention, which is whether or not the susceptibility anisotropy, the surface energies, and the elastic constants depend on the strength of the electric field. In principle, they do. The reason is that these quantities depend on the level of alignment of the particles in the coexisting isotropic and nematic phases [35,48–50]. We also note that, strictly speaking, the isotropic phase becomes paranematic in the presence of an alignment field. In fact, the isotropic-to-nematic phase transition ends in a critical point, at which both the interfacial tension and anchoring should vanish [6,51–53]. To keep our analysis as simple as possible, and within the philosophy of linear response theory, we shall ignore any impact of the electric field on the elastic constants and surface energies, and presume the external field in some sense to be sufficiently weak not to affect these quantities, yet sufficiently strong to deform the tactoids.

To find the equilibrium shape and director field configuration of tactoids, we would need to solve the appropriate Euler-Lagrange equations that result from a minimization of the free energy, given in Eq. (1). The minimization is with respect to the director field $\vec{n}(\vec{r})$, which depends on the spatial coordinate $\vec{r}$ as well as on the droplet shape. This has to be done subject to the conditions of a constant droplet volume and a constant unit length of the director, $|\vec{n}| \equiv 1$ [42], which produces a quite complex mathematical problem, also numerically, in view of the free boundary [28,37].

Hence, we follow the earlier work of Kaznacheev *et al.* [26,27] and Prinsen *et al.* [28–30], and restrict the geometry of both the director field and droplet shape. For the shapes of the droplets we use circle sections rotated about their chord, producing potentially elongated droplets with sharp ends that are very similar to the tactoid shapes found in a wide variety of experiments, including those of Metselaar *et al.* [39]. We are aware that the equilibrium shape of the poles is a cusp if

$0 \leqslant \omega < 1$ and the director field (nearly) uniform, which in that case has a more rounded form. However, as we showed in [28], the free energy difference between the exact Wulff shape, the spindle shape, and ellipsoids of revolution is minute for $\omega < 1$, so we deem the approximation not to be a grave one.

For the director field we employ a bispherical coordinate system first used by Williams to describe spherical bipolar droplets [37], and more recently by Prinsen *et al.* [28–30], Jamali *et al.* [5,12], and Kaznacheev *et al.* [26,27] for elongated bipolar droplets. We do not fix the position of the foci of the bispherical director field to the poles of the tactoid to allow for a smooth interpolation between a uniform and bipolar director field, although we do prescribe them to reside on the main axis of revolution of the tactoid. See also Fig. 2.

Within this prescription, the shape and director field configuration of a tactoid is completely described by two parameters, at least if the volume of the droplet is known. These two parameters are the opening angle α and the ratio $y \equiv \tilde{R}/R$ of the distance between the virtual boojums, $2\tilde{R}$, and length of the droplet, $2R$. The former quantity describes the aspect ratio $x \equiv R/r = \cot(\alpha/2)$ of the droplet, with r the half-width of the droplet, and the latter the degree of "bipolarness" of the director field. For a spherical droplet, we have $x = 1$ and $\alpha = \pi/2$, while for a strongly elongated one $x \gg 1$ and $\alpha \ll 1$. For a tactoid with a uniform director field $y \gg 1$, and for a bipolar tactoid $y \to 1$, see also Fig. 2. We note that the quantities x and y will explicitly contribute to the scaling theory presented in the following section.

It turns out practical to render the free energy dimensionless, and define $f = f(\alpha, y) \equiv \sigma F/(K_{11} - K_{24})^2$. The optimal free energy minimizes f with respect to the opening angle α or aspect ratio x and the bipolarness y, keeping the volume V of the droplet constant. Let the dimensionless volume be defined as $v \equiv V[(\sigma/(K_{11} - K_{24})]^3$. The dimensionless free energy f can then be written as a sum of surface and volume terms

$$\begin{aligned} f(\alpha, y) = {} & v^{2/3}\phi_{\mathrm{v}}^{-2/3}(\alpha)[\phi_\sigma(\alpha) + \omega\phi_\omega(\alpha, y)] \\ & + v^{1/3}\phi_{\mathrm{v}}^{-1/3}(\alpha)[\phi_{11}(\alpha, y) + \kappa\phi_{33}(\alpha, y)] \\ & - v\phi_{\mathrm{v}}^{-1}(\alpha)\Gamma\phi_{\mathrm{C}}(\alpha, y), \end{aligned} \tag{5}$$

where we refer to the Supplemental Material (SM) [54] for details. The first line represents the two surface contributions, the second line corresponds to the three types of elastic deformation of the director field, and the last is related to the Coulomb energy. Here, $\kappa \equiv K_{33}/(K_{11} - K_{24})$ measures the magnitude of the bend elastic constant relative to the effective splay constant, and $\Gamma = \frac{1}{8\pi}\epsilon_a E^2 \sigma^{-2}(K_{11} - K_{24})$ is the appropriate quantity to probe the impact of the electric field relative to the surface tension and elastic deformation.

For the case of lyotropic nematics of rodlike particles, we typically have $\sigma \approx 10^{-7}$–10^{-6} N m^{-1} for the surface tension [55], and $K_{33}/K_{11} \approx 1$–10^2 and $K_{11} \approx 10^{-12}$–10^{-11} N for the elastic constants [12,28,56–58]. Dimensionless anchoring strengths ω are typically in the range from about 1 to 10 [5,11,27,29].

All three terms are renormalized by a function measuring how the opening angle α affects the droplet volume for a given aspect ratio x. The common factor is given by

$$\phi_{\mathrm{v}}(\alpha) = \frac{7\pi}{3} + \frac{\pi}{2}\left(\frac{1 - 4\alpha\cot\alpha + 3\cos 2\alpha}{\sin^2\alpha}\right). \tag{6}$$

The first line of Eq. (5) consists of the sum of a contribution from the bare surface tension,

$$\phi_\sigma(\alpha) = 4\pi\left(\frac{1 - \alpha\cot\alpha}{\sin\alpha}\right), \tag{7}$$

and a term originating from the anchoring of the director field to the interface,

$$\begin{aligned} \phi_\omega(\alpha, y) = {} & \frac{\pi}{2}(y^2 - 1)^2 \sin^3\alpha \\ & \times \int_0^\pi d\xi \left[\frac{\sin^2\xi\cos^2\xi}{N(y, \xi, \alpha)(1 + \sin\xi\cos\alpha)^3}\right], \end{aligned} \tag{8}$$

for which we have not been able to obtain an explicit expression. Here,

$$\begin{aligned} N(y, \xi, \eta) = {} & \left(\sin\xi\cos\eta + \tfrac{1}{2}Z(\xi, \eta)(y^2 - 1)\right)^2 \\ & + y^2\sin^2\xi\sin^2\eta \end{aligned} \tag{9}$$

and

$$Z(\xi, \eta) = 1 + \sin\xi\cos\eta. \tag{10}$$

Note that in Eq. (8), we inserted $\eta = \alpha$ to obtain the expression for N in Eq. (9).

The contribution of the splay and saddle-splay deformation to the Frank elastic energy also gives rise to an integral that we have also not been able to solve analytically:

$$\begin{aligned} \phi_{11}(\alpha, y) = {} & 8\pi \int_0^\pi d\xi \int_0^\alpha d\eta\ \sin^2\xi\cos^2\xi\ \sin\eta \\ & \times \frac{1}{N(y, \xi, \eta)(1 + \sin\xi\ \cos\eta)^3}, \end{aligned} \tag{11}$$

where we note that within our family of bispherical director fields, the saddle-splay deformation merely renormalizes the contribution from the splay deformation, giving rise to an effective splay constant that is the difference of the splay and bend-splay constants, explaining the scaling of the free energy that we introduced above in terms of this difference [28,29]. The contribution of the bend elastic deformation reads as

$$\begin{aligned} \phi_{33}(\alpha, y) = {} & 8\pi \int_0^\pi d\xi \int_0^\alpha d\eta\ \sin^4\xi\ \sin^3\eta \\ & \times \frac{1}{N(y, \xi, \eta)(1 + \sin\xi\ \cos\eta)^3}. \end{aligned} \tag{12}$$

Finally, the free energy of the interaction of the nematic droplet with an electric field yields an even more daunting integral

$$\begin{aligned} \phi_{\mathrm{C}}(\alpha, y) = {} & 8\pi \int_0^\pi d\xi \int_0^\alpha d\eta \frac{\sin^2\xi\sin\eta}{(1 + \sin\xi\ \cos\eta)^3} \\ & \times \frac{(y^2Z^2 + \sin^2\xi\ \sin^2\eta - \cos^2\xi)^2}{N(y, \xi, \eta)(1 + \sin\xi\ \cos\eta)^2}. \end{aligned} \tag{13}$$

Details of the derivation of all these expressions can be found in the SM [54].

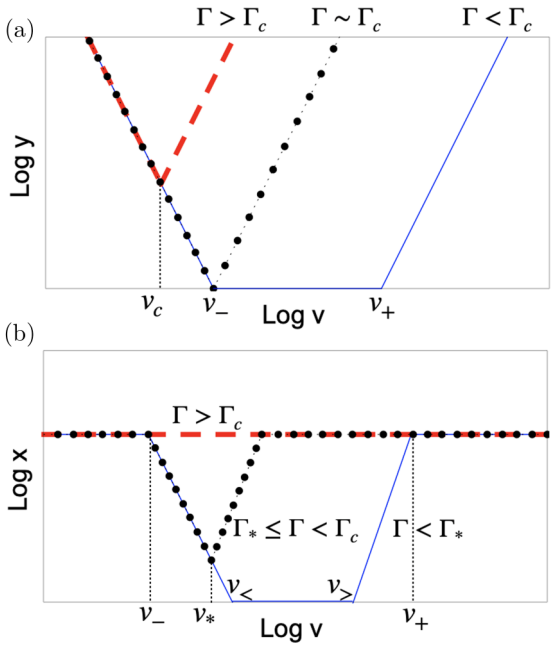

FIG. 3. Dependence of (a) the degree of bipolarness y and (b) the aspect ratio x of tactoids on the scaled volume v in the presence of an electric field, according to the scaling theory. Blue solid line: the field strength Γ is below the critical value Γ_c, and the anchoring strength ω is somewhat larger than unity. The volumes v_- and v_+ demarcate crossovers from quasibipolar director fields to bipolar ones, and $v_<$ and $v_>$ those from elongated to spherical droplet shapes. Dashed-dotted line: same curve, but now for $\Gamma = \Gamma_c$. Dashed lines: $\Gamma > \Gamma_c$. For fields above the critical field strength Γ_*, the tactoids are always elongated provided the anchoring strength ω is sufficiently large. See the main text. The slopes of the various curves are listed in Tables I, II, and III, and the values of the various crossover volumes and field strengths in Table IV.

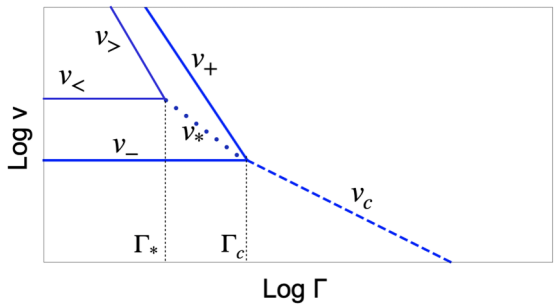

FIG. 4. Schematic "phase" diagram of director fields of tactoids in an external field. Plotted is the scaled volume v versus the scaled field strength Γ. Indicated are the crossovers between the five regimes, demarcated by the crossover volumes v_-, v_+, $v_<$, $v_>$, v_*, and v_c. Expressions for the crossover volumes v_-, v_+, $v_<$, and $v_>$, and the critical field strengths Γ_c and Γ_*, are listed in Table IV. See also the main text. In the region bounded by v_- and v_c, tactoids with sufficiently large anchoring strength $\omega \gg 1$ are elongated with a director field that is quasibipolar with a bipolarness y that decreases with increasing volume. In the region bounded by v_c and v_+ in the upper right-hand corner it is quasibipolar with a bipolarness that increases with droplet volume. In region bounded by v_- and v_+ in the upper left-hand corner. the director field is for all intents and purposes bipolar. The tactoids are more or less spherical in the region bounded by $v_<$ and $v_>$ in the uppermost left-hand corner, and elongated outside of that region, at least if $\omega \gg 1$. The volume v_c demarcates the crossover from decreasing to increasing bipolarness for quasibipolar director fields, the volume v_* that between decreasing aspect ratio to increasing aspect ratio.

The various integrals can be solved explicitly for the cases $y = 1$ and $y \to \infty$, but so far have eluded analytical evaluation for the general case $y \geqslant 1$ [26,28]. Hence, we need to take recourse to a numerical evaluation and minimization with respect to the opening angle α and the bipolarness y. We recall that there is a one-to-one mapping between the opening angle α and the aspect ratio x of the tactoids. From Eq. (5) we deduce that our parameter space is quite substantial: (i) the scaled volume of the droplets v, (ii) the dimensionless anchoring strength ω, (iii) the ratio of the bend and splay elastic constants κ, and (iv) the dimensionless strength of the magnetic field Γ.

Before numerically solving the pertinent equations in Sec. IV, we first analyze in Sec. III the problem from the perspective of scaling theory for (nearly) spherical and (highly) elongated droplets. This allows us to demarcate the crossovers between the various parameter regimes, and find the scaling exponents relevant to the behavior of the droplet shape and director field. As we shall see in Sec. IV, our scaling theory and our variational theory are consistent with each other.

For those not interested in the full scaling analysis, which is rather technical in nature and details transitions between no fewer than five regimes, we refer to Figs. 3 and 4 that summarize our main findings. The scaling relations that we find are summarized in Tables I, II, and III, and Table IV lists all crossover volumes and external field strengths.

III. SCALING THEORY

Rather than getting the exact expression for the free energy (5), we may also estimate the equilibrium shape and director field configuration of a tactoid by applying simple geometric arguments or resorting to asymptotic relations valid for the various integrals that we introduced in the preceding section. We assume that the droplet looks like a spindle with the short axis r and the long axis $R \geqslant r$, and that its director field is quasibipolar, i.e., the director field converges outside the droplet to virtual point defect or boojums (see Fig. 2). The (half) distance between the (virtual) defects is $\tilde{R} \geqslant R$.

Referring to the free energy functions (1)–(4), we notice that the elastic and electric-field contributions must be proportional to the droplet volume $V \propto Rr^2$, while the surface contributions must be proportional to the area of the droplet $S \propto rR$. Following Prinsen *et al.* [29], we argue that the radius of curvature of a bend deformation must scale as $\tilde{R}^2/r$ and that of the splay as $\tilde{R}^2/R$. Furthermore, the anchoring strength term, proportional to $(\vec{q} \cdot \vec{n})^2$, scales as $(r^2/R^2)(1 - R^2/\tilde{R}^2)^2$ [12,29], as we in fact also show in the SM. Finally, the field term $(\vec{E} \cdot \vec{n})^2$ is proportional to $E^2 r^2 R^2/\tilde{R}^4$.

As already alluded to in the previous section, there are two quantities that a nematic droplet can optimize in order to lower its free energy: the aspect ratio $x = R/r \geqslant 1$ and the bipolarness $y = \tilde{R}/R \geqslant 1$. The dimensionless free energy of a

TABLE I. Summary of the various scaling regimes for the bipolarness y of nearly spherical tactoids ($x \simeq 1$) in the presence and absence of an electric field, for large, intermediate, and small droplet sizes v, relative to the crossover volumes v_- and v_+. If the electric field is weak and $0 < \Gamma < \Gamma_c$, the bipolarness of the droplet has three different regimes. Under a strong field, $\Gamma > \Gamma_c$ there are two regimes. Expressions for the crossover volumes v_- and v_+ and the critical field strength Γ_c are listed in Table IV. Notice that for $\Gamma = 0$, $v_+ \to \infty$ and there are strictly speaking only two regimes.

	$v < v_-$	$v_- < v < v_c$	$v_c < v < v_+$	$v > v_+$
$\Gamma < \Gamma_c$	$y \sim \omega^{-1/2} v^{-1/6} (1+\kappa)^{1/2}$	$y \sim 1$	$y \sim 1$	$y \sim \Gamma^{1/2} \omega^{-1/2} v^{1/6}$
$\Gamma > \Gamma_c$	$y \sim \omega^{-1/2} v^{-1/6} (1+\kappa)^{1/2}$	$y \sim \omega^{-1/2} v^{-1/6} (1+\kappa)^{1/2}$	$y \sim \Gamma^{1/2} \omega^{-1/2} v^{1/6}$	$y \sim \Gamma^{1/2} \omega^{-1/2} v^{1/6}$

droplet with aspect ratio x and bipolarness y reads as within our scaling ansatz

$$f(x,y) \sim v^{2/3} x^{1/3} [1 + \omega x^{-2}(1-y^{-2})^2] + v^{1/3} y^{-4} x^{-4/3} (1 + \kappa x^{-2}) + \Gamma v x^{-2} y^{-4}, \quad (14)$$

where we have ignored all constants of proportionality. The values of the dimensionless anchoring strength ω, bend constant $\kappa = K_{33}/(K_{11} - K_{24})$, electric-field strength $\Gamma = \frac{1}{8\pi} \sigma^{-2} \epsilon_a E^2 (K_{11} - K_{24})$, and volume $v \equiv V\sigma^3/(K_{11} - K_{24})^3$ determine what values of x and y minimize the free energy f. The first term in Eq. (14) represents the surface free energy, the second term the elastic deformation, and the last term the interaction of the droplet with the external electric field. Notice that the various terms can also be derived from Eq. (1) by applying a formal expansion for small $\alpha \simeq x^{-1}$, and keeping only the leading order term of each contribution. We refer to the SM for details.

As we shall see, there are always two terms that dominate the shape and director field of a tactoid: either the surface and elastic energy, or the surface and Coulomb energy. This is a result of the different scaling with the dimensionless volume v: $v^{1/3}$ for the elastic free energy, $v^{2/3}$ for the interfacial free energy, and v for the Coulomb free energy. This means that droplet size crucially determines the shape and director field behavior of tactoids.

It is important to note at this point that the specific form of our scaling ansatz for the free energy [Eq. (14)] automatically ensures that $y \geqslant 1$ but not that $x \geqslant 1$. The former follows directly from the observation that the first term has a minimum for $y = 1$, while all the other terms decrease as $y > 0$ increases. Further, Eq. (14) does *not* hold for lens-shaped tactoids, that is, for $x < 1$. Indeed, the surface free energy for $x \ll 1$ would require a term proportional to an area that scales as r^2 rather than the Rr that is valid for $x \geqslant 1$. Similar arguments hold for the elastic and Coulomb terms [32,59,60].

In order to deal with the fact that our free energy does not automatically ensure the condition that $x \geqslant 1$ for $\omega \geqslant 0$, we have to separate the case of elongated droplets with $x \gg 1$ from that of spheroidal droplets with $x \approx 1$. In fact, for $\omega < 0$ the tactoids become lens shaped with $x < 1$, a case we do not consider in this work as it has been dealt with elsewhere [32,59,60]. The case $x \approx 1$ can be investigated by putting $x = 1$ in the free energy, and not optimizing with respect to both x and y, but only with respect to y. The crossover from elongated to spheroidal emerges automatically from our analysis, as we shall see. In what follows, we first analyze the the simpler case for which the aspect ratio is close to unity, and next consider the case where the aspect ratio is significantly larger than unity.

A. Nearly spherical tactoids

As we shall see in the next subsection, tactoids are always nearly spherical if the anchoring strength ω is about unity or smaller [see Eq. (3)], irrespective of the value of the scaled volume v and that of the scaled strength of the electric field Γ. If $\omega \gg 1$, then the droplets become spherical only for a range of volumes that we will specify below, and then only if the field strength is below some critical value.

Minimizing the free energy $f(1,y)$ for nearly spherical droplets with respect to the bipolarness y, we find for its optimal value

$$y^2 \simeq 1 + \omega^{-1}(1+\kappa) v^{-1/3} + \Gamma \omega^{-1} v^{1/3}. \quad (15)$$

This expression immediately highlights the importance of the volume of the droplet. The director field is uniform, corresponding to $y \gg 1$, either if $\omega^{-1}(1+\kappa)v^{-1/3} \gg 1$ or $\Gamma\omega^{-1}v^{1/3} \gg 1$. In other words, if $v \ll v_- = \omega^{-3}(1+\kappa)^3$ or $v \gg v_+ = \omega^3\Gamma^{-3}$. For droplet volumes $v_- \leqslant v \leqslant v_+$, the director field is (quasi)bipolar, and $y \approx 1$.

Thus, we find that there are potentially three different regimes and two critical volumes that dictate the behavior of the droplet. For $v \ll v_-$, we obtain the scaling relation

$$y \sim v^{-1/6} \omega^{-1/2} (1+\kappa)^{1/2}, \quad (16)$$

TABLE II. This table summarizes the various scaling regimes for the bipolarness y of elongated tactoids ($x \gg 1$) in the presence and absence of an electric field, for large, intermediate, and small droplet sizes v, relative to the crossover volumes v_- and v_+. If the electric field is weak and $0 < \Gamma < \Gamma_c$, the bipolarness of the droplet has three different regimes. Under a strong field, $\Gamma > \Gamma_c$ there are two regimes. Expressions for the crossover volumes v_- and v_+, and the critical field strength Γ_c, are listed in Table IV. Notice that for $\Gamma = 0$, $v_+ \to \infty$ and there are strictly speaking only two regimes.

	$v < v_-$	$v_- < v < v_c$	$v_c < v < v_+$	$v > v_+$
$\Gamma < \Gamma_c$	$y \sim \omega^{-5/12} v^{-1/6} (1+\kappa\omega^{-1})^{1/2}$	$y \sim 1$	$y \sim 1$	$y \sim \Gamma^{1/2} \omega^{-7/12} v^{1/6}$
$\Gamma > \Gamma_c$	$y \sim \omega^{-5/12} v^{-1/6} (1+\kappa\omega^{-1})^{1/2}$	$y \sim \omega^{-5/12} v^{-1/6} (1+\kappa\omega^{-1})^{1/2}$	$y \sim \Gamma^{1/2} \omega^{-7/12} v^{1/6}$	$y \sim \Gamma^{1/2} \omega^{-7/12} v^{1/6}$

TABLE III. This table summarizes the various scaling regimes for the aspect ratio x of tactoids in the presence and absence of an electric field, for large, intermediate, and small droplet sizes v, relative to the crossover volumes v_- and v_+, and $v_<$ and $v_>$. For simplicity, we have dropped any dependence of the aspect ratio on κ. Expressions for the crossover volumes v_-, v_+, $v_<$, and $v_>$, and the critical field strengths Γ_c and Γ_* are listed in Table IV. Notice that for $\Gamma = 0$, $v_+ \to \infty$, and $v_> \to \infty$.

	$v < v_-$	$v_- < v < v_<$	$v_< < v < v_*$	$v_* < v < v_>$	$v_> < v < v_+$	$v > v_+$
$\Gamma < \Gamma_*$	$x \sim \sqrt{\omega}$	$x \sim v^{-1/5}$	$x \sim 1$	$x \sim 1$	$x \sim \Gamma^{3/7} v^{1/7}$	$x \sim \sqrt{\omega}$
$\Gamma_* < \Gamma < \Gamma_c$	$x \sim \sqrt{\omega}$	$x \sim v^{-1/5}$	$x \sim v^{-1/5}$	$x \sim \Gamma^{3/7} v^{1/7}$	$x \sim \Gamma^{3/7} v^{1/7}$	$x \sim \sqrt{\omega}$
$\Gamma > \Gamma_c$	$x \sim \sqrt{\omega}$	$x \sim \sqrt{\omega}$	$x \sim \sqrt{\omega}$	$x \sim \sqrt{\omega}$	$x \sim \sqrt{\omega}$	$x \sim \sqrt{\omega}$

while for $v \gg v_+$, we have

$$y \sim v^{1/6} \Gamma^{1/2} \omega^{-1/2}. \tag{17}$$

Notice that the exponents of $-\frac{1}{6}$ for volumes $v \ll v_-$ and of $+\frac{1}{6}$ for $v \gg v_+$ are universal. A summary of these results is given in Table I.

We notice that as the electric-field strength increases, v_+ decreases and the two critical volumes merge into one critical volume: $v_- = v_+$. This happens at a critical electric field $\Gamma_c \simeq \omega^2 (1+\kappa)^{-1}$. If $\Gamma \geqslant \Gamma_c$, the bipolarness y is always greater than unity for any size of the droplet, and the droplet is never fully bipolar. The crossover of a decreasing bipolarness to an increasing one with increasing volume then happens at a critical volume $v_c = \omega^{-3}(1+\kappa)^3$, where we inserted Γ_c in the expression for v_+. If $\Gamma > \Gamma_c$, we find the crossover to occur for $v_c = \Gamma^{-3/2}(1+\kappa)^{3/2}$ that can be found by equating Eqs. (16) and (17). The summary of the results of this subsection is presented in Table I.

So, in conclusion, if $\Gamma > \Gamma_c$, then $y \gg 1$ decreases with increasing volume v of the tactoid until larger than the critical value v_c. If larger than v_c, y increases again with increasing volume and y does not approach the value of unity, that is, the tactoid does not become bipolar. For $\Gamma < \Gamma_c$, the director field is bipolar if $v_- < v < v_+$, but not outside of this range of volumes. For $v < v_-$ the bipolarness y decreases with increasing volume, while for $v > v_+$ it increases with increasing volume. All in all, this demarcates three scaling regimes for the degree of bipolarness of the director field.

As we shall see next, for elongated tactoids the number of regimes increases to five.

TABLE IV. Listing of all crossover volumes v and critical field strengths Γ, for small and large values of the anchoring strength ω. Crossovers form elongated to spherical tactoids only occur if ω is sufficiently large.

	$\omega \leqslant 1$	$\omega \geqslant 1$
v_-	$\omega^{-3}(1+\kappa)^3$	$\omega^{-5/2}(1+\kappa\omega^{-1})^3$
v_+	$\omega^3 \Gamma^{-3}$	$\omega^{7/2}\Gamma^{-3}$
v_c	$\Gamma^{-3/2}(1+\kappa)^{3/2}$	$\Gamma^{-3/2}\omega^{-1}(1+\kappa\omega^{-1})^{3/2}$
$v_<$	–	$(1+\kappa)^3$
$v_>$	–	Γ^{-3}
v_*	–	$\Gamma^{-5/4}$
Γ_*	–	$(1+\kappa)^{-1}$
Γ_c	$\omega^2(1+\kappa)^{-1}$	$\omega^2(1+\omega^{-1}\kappa)^{-1}$

B. Elongated tactoids

For elongated tactoids, matters become significantly more complex. To calculate the optimal values for the bipolarness y and the aspect ratio x for $x \gtrsim 1$, we need to minimize the free energy (14) with respect to both x and y. This gives rise to the following set of coupled equations:

$$y^4 = \omega x^{-2}(y^2-1)^2 + v^{-1/3}x^{-5/3}(1+\kappa x^{-2}) + v^{1/3}\Gamma x^{-7/3} \tag{18}$$

and

$$y^2 = 1 + \omega^{-1}x^{1/3}(1+\kappa x^{-2})v^{-1/3} + \Gamma\omega^{-1}v^{1/3}x^{-1/3}. \tag{19}$$

Inserting the last two terms of Eq. (19) in Eq. (18), we find

$$\frac{x^2}{\omega} = (1-y^{-2}) + (1-y^{-2})^2. \tag{20}$$

Inserting this back in Eq. (19) produces a nonlinear equation entirely in terms of the quantity y. Unfortunately, we have not been able to solve this expression exactly. It can of course be solved numerically, but this would obviously defeat the purpose of the scaling theory. Fortunately, the governing equations can be solved asymptotically in a number of useful limiting cases that we will discuss next.

For instance, we have seen in the preceding section that for very large and very small droplet volumes the director field must be nearly homogeneous, implying that $y \gg 1$. We note that large and small here refer to the critical volumes v_- and v_+, introduced already in the preceding subsection for nearly spherical tactoids but that now will conform to slightly different expressions given below. Equation (20) tells us that if $y \to \infty$, the director field is uniform, and the aspect ratio is (apart from a multiplicative constant) equal to $\sqrt{\omega}$. This is consistent with the exact result $x = 2\omega^{1/2}$ obtained by means of the Wulff construction for $\omega \gg 1$ [28].

Inserting $x \simeq \omega^{1/2}$ in Eq. (18) gives, to leading order for large values of y,

$$y^2 \sim v^{-1/3}\omega^{-5/6}(1+\kappa\omega^{-1}) + v^{1/3}\omega^{-7/6}\Gamma. \tag{21}$$

This means that for sufficiently small droplets

$$y \sim v^{-1/6}\omega^{-5/12}(1+\kappa\omega^{-1})^{1/2}, \tag{22}$$

while if they are sufficiently large we have

$$y \sim v^{1/6}\omega^{-7/12}\Gamma^{1/2}. \tag{23}$$

It is worth mentioning that the result for large droplets does *not* depend on the value of κ that is a measure for the

magnitude of the bend elastic constant. Recall that in Eqs. (16) and (17), we find the same scaling of the bipolarness with the dimensionless volume for nearly spherical droplets. The scaling with the anchoring strength is slightly different, however.

Equation (22) applies for $v \ll v_- = \omega^{-5/2}(1+\kappa\omega^{-1})^3$ and Eq. (23) for $v \gg v_+ = \Gamma^{-3}\omega^{7/2}$, as can be deduced from Eq. (21). These critical volumes differ slightly from those we calculated for nearly spherical tactoids, as already announced. We conclude that if $v_- \leqslant v \leqslant v_+$ the elongated droplets must be bipolar.

If v_+ drops below v_-, the tactoids are always more or less uniform, and $x \simeq \omega^{1/2}$. This happens at a critical field strength $\Gamma_c = \omega^2(1+\kappa\omega^{-1})$ that we find by setting $v_+ = v_-$. The crossover of decreasing to increasing bipolarness with increasing volume now occurs at a critical volume $v_c = \omega^{-3}$ for $\Gamma = \Gamma_c$. If $\Gamma > \Gamma_c$, the crossover happens at a critical volume $v_c = \Gamma^{-3/2}\omega^{1/2}(1+\kappa\omega^{-1})^{3/2}$, which we find by equating Eqs. (22) and (23).

What the aspect ratios of the tactoids are when $v_- \leqslant v \leqslant v_+$, so when the director field is no longer uniform, can be inferred from Eqs. (19) by inserting $y = 1+\delta$ in Eq. (20) and presuming that $\delta \ll 1$. Solving these equations then gives to leading order in $\delta = x^2\omega^{-1} \ll 1$ an expression for the aspect ratio: $x^{5/3} \sim v^{-1/3}(1+\kappa x^{-2}) + v^{1/3}\Gamma x^{-2/3}$. For small droplets with a volume $v_+ \gg v > v_-$, we have $x \sim v^{-1/5}$ if we ignore the contribution from the bend elasticity; thus, the droplet becomes less elongated with increasing volume. For larger ones $v_- \ll v < v_+$, the aspect ratio $x \sim v^{1/7}\Gamma^{3/7}$ grows again with increasing volume.

As we need to insist that $x > 1$ for the equations to hold, we take the value of $x = 1$ as the crossover to the regimes where the droplets are more or less spherical. Inserting this condition in the equation for the aspect ratio gives $1 \sim v^{-1/3}(1+\kappa) + v^{1/3}\Gamma$, which we translate in two crossover volumes. In the absence of a field, the crossover from an elongated droplet with $x = \omega^{1/2}$ to a nearly spherical droplet with $x = 1$ occurs for $v = v_<$ with $v_< \equiv (1+\kappa)^3 > v_-$ another crossover volume. For sufficiently weak fields, they start to elongate again if $v_> < v < v_+ = \Gamma^{-3}\omega^{7/2}$ with the crossover volume $v_> \equiv \Gamma^{-3}$ smaller than v_+ since we presume that $\omega > 1$. For $v > v_+$ the director field is uniform and the aspect ratio obeys again $x \sim \omega^{1/2}$.

The picture that emerges is one where for $v < v_-$ the nematic droplets have a more or less uniform director field with an aspect ratio of about $\omega^{1/2}$, and the same for $v > v_+$. If $v > v_-$, the droplets become increasingly bipolar and the aspect ratio decreases with increasing volume. If the scaled volume v increases further to get closer to v_+, the bipolar character of the director field diminishes again with increasing volume, while the aspect ratio increases to its maximum value of about $\omega^{1/2}$ (see Fig. 3). Notice that we have presumed that $\omega \gg 1$; otherwise, we would not have $x \gg 1$.

Somewhere in the size range $v_- \leqslant v \leqslant v_+$, the droplets actually become nearly spherical, in which case the theory of the preceding section applies. This happens in the range of volumes for which $v_< < v < v_>$. The nearly spherical drop regime disappears if $v_< = v_>$. Equating these critical volumes shows that this occurs for field strengths Γ larger than the critical value of $\Gamma_* \equiv (1+\kappa)^{-1}$. In that case, we only have crossover from decreasing elongated to increasing elongated at a crossover volume $v_* = \Gamma^{-5/4}$. Since $\Gamma_* < \Gamma_c$, we conclude that for $\omega \gg 1$ we lose the spherical tactoid regime before we lose the bipolar director field.

The summaries of these results are presented in Tables II, III, and IV, as well as in Fig. 4, showing the different regimes and crossovers. The conclusion of our scaling theory is that the aspect ratio of the nematic droplets is at most $\omega^{1/2}$, independent of the volume or the field strength. In other words, external fields cannot elongate a tactoid to aspect ratios beyond those that are found in the absence of a field, at least for the family of director fields that we presume. We return to this issue in the Discussion section below.

In the next section, we present the numerical evaluation of our variational theory and obtain the mathematically exact response of the director field and the shape of the droplet in the presence of an electric field, and compare these with the scaling theory. As we shall see, our scaling predictions are robust. This means also that the conclusions that we base them on are robust.

IV. NUMERICAL RESULTS

The scaling theory of the preceding section has enabled us to identify different scaling regimes, which we now investigate by numerically minimizing the free energy (5). To this end, we evaluate Eq. (5) for opening angles $0 \leqslant \alpha \leqslant \pi$ and degrees of bipolarness of the director field $1 \leqslant y \leqslant \infty$ and find the values of these quantities for which the free energy f is minimal. So, for a given scaled volume v, anchoring strength ω, ratio of bend-to-splay elastic constants κ and electric field strength Γ, we obtain the optimal values of both α and y. We recall that the aspect ratio of the tactoids x is directly linked to the opening angle via the relation $x = \cot(\alpha/2)$. In order to find the minimum free energy, we numerically calculate all integrals given in Sec. II.

It is clear that the electric field drives the director field to align itself with it, implying that the major axis of a tactoid orients parallel to the electric field. This happens irrespective of whether the director field configuration is uniform or bipolar. If the electric field is sufficiently weak, the director field is not perturbed by the electric field. If the field is sufficiently strong, we would expect the director field of the droplet to become homogeneous, even if the director field in the absence of a field is bipolar. What weak and strong here mean depends on volume of a tactoid as we have seen in the preceding section, and is schematically summarized in Figs. 3 and 4.

Figure 5 confirms this expectation. Shown is the bipolarness y as a function of the dimensionless volume v of the tactoids, for the case where we (arbitrarily) set for the dimensionless bend constant $\kappa = 10$ and for the anchoring strength $\omega = 14$. Indicated are results for different values of the dimensionless electric field Γ. We confirm the scaling prediction that two critical volumes emerge, one associated with the crossover from a quasibipolar to a bipolar director field v_-, and one with the crossover from a bipolar to quasibipolar director field v_+. For $\Gamma \geqslant 100$, we only find quasibipolar director fields characterized by a bipolarness $y > 1$ for all volumes v. The scaling exponent β we find for $y \sim v^\beta$ equals $\beta = -0.15$ for small volumes and $\beta = +0.16$ for large volumes, values that agree reasonably well with the predicted

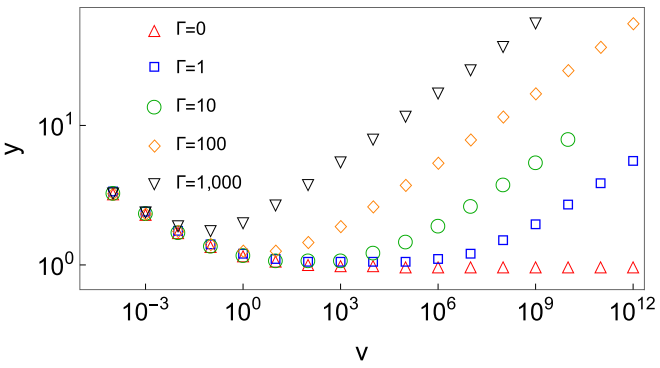

FIG. 5. The bipolarness y of the director field of a tactoid in the presence of an electric field as a function of its dimensionless volume v. Indicated by the different symbols are results for different values of the dimensionless electric-field strength Γ. The dimensionless anchoring strength is fixed at $\omega = 14$ and the dimensionless bend constant at $\kappa = 10$.

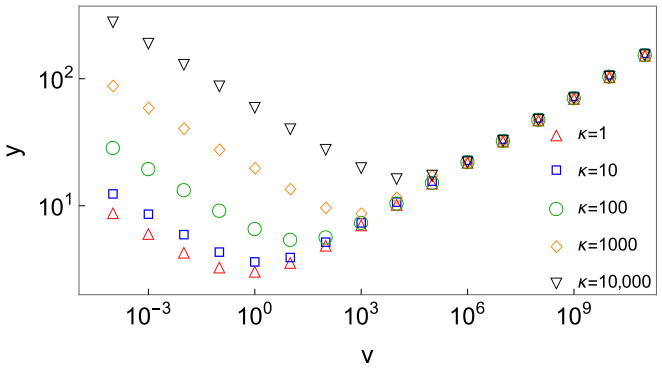

FIG. 7. Bipolarness y of the droplet as a function of the dimensionless volume v of tactoids in the presence of an electric field for different values of the dimensionless bend constants κ indicated by the symbols. Anchoring strength $\omega = 14$ and dimensionless field strength $\Gamma = 100$.

exponents of $-\frac{1}{6}$ and $+\frac{1}{6}$ that we obtained from the scaling theory and are quoted in Table II.

Figure 5 also shows that the bipolarness y increases with the electric-field strength Γ, if the volume of a tactoid is sufficiently large $v > v_+$. According to the scaling prediction (23), y should scale as $\Gamma^{1/2}$. Figure 6, in which we plotted the bipolarness as a function of the field strength for the case where $\omega = 14$ and $\kappa = 10$, confirms that the scaling exponent is 0.5 over three decades of Γ. So, indeed, increasing the field strength leads to director fields that become increasingly homogeneous, as one would in fact expect from the scaling theory of the previous section. See also Table II.

According to the scaling theory of the preceding section, the impact of the (scaled) bend elastic constant κ on the bipolarness y of a tactoid is negligible for sufficiently large tactoids in the presence of an external field. See Table II. It is negligible for small tactoids too, but only provided $\kappa \ll \omega$. Our numerical results presented in Fig. 7 confirm for the case $\omega = 14$, the bipolarness is an invariant of κ for sufficiently large volumes, but becomes a function of κ for values larger than about 10, as expected from the scaling theory.

For bend elastic constants $\kappa > 10 \approx \omega$, the bipolarness should exhibit a power-law scaling predicted by the scaling relation (22) that then takes the simpler form $y \sim v^{-1/6}\omega^{-11/12}\kappa^{1/2}$. In Fig. 8 we have plotted the bipolarness y as a function of κ for $\Gamma = 100$ and $v = 10^{-4}$. The exponent that we measure is 0.49, which is indeed close to the value obtained from the scaling theory. Our scaling theory also predicts the bipolarness of the tactoids to depend on the anchoring strength ω. Indeed, Eqs. (16) and (17) for nearly spherical tactoids, and Eqs. (22) and (23) for elongated ones, predict that both for small and large droplets the bipolarness should shift with shifting anchoring strength. This makes intuitive sense because the larger the anchoring strength is, the larger the free energy penalty becomes for imperfect planar anchoring. Hence, with increasing anchoring strength the tactoids should become increasingly bipolar. This is what our numerical calculations also confirm, as is shown in Fig. 9. On a logarithmic scale, the curves shift vertically by an amount that depends on the anchoring strength ω.

The scaling of the bipolarness y with the anchoring strength ω is highly nontrivial, as is implicit in the scaling predictions (16) and (17) for nearly spherical tacoids, and Eqs. (22) and (23) for elongated ones. It depends not only on the shape of the tactoids, but also whether the tactoids are large or small, and on whether or not the bend elastic constant is large. To account for this, we plot in Figs. 10 and 11 the bipolarness y as a function of the anchoring strength ω for two droplet sizes and fixed values of $\Gamma = 10$ and $\kappa = 0$. The appropriate scaling

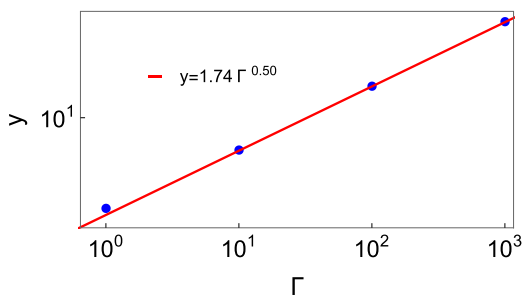

FIG. 6. Bipolarness y of a tactiod as a function of the dimensionless electric field Γ for a dimensionless volume $v = 10^7$. Anchoring strength $\omega = 14$ and dimensionless bend constant $\kappa = 10$. The solid line shows the scaling of y as with $\Gamma^{0.5}$.

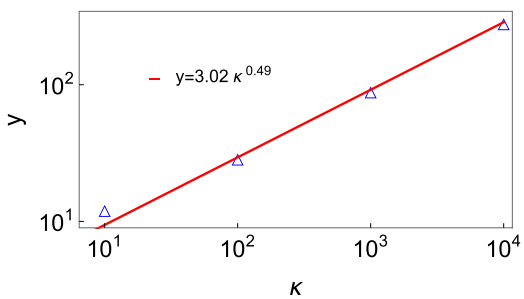

FIG. 8. Bipolarness of a tactoid as a function of the dimensionless bend constant κ in the presence of an electric field. Anchoring strength $\omega = 1.4$, dimensionless field strength $\Gamma = 100$, and dimensionless volume $v = 10^{-4}$.

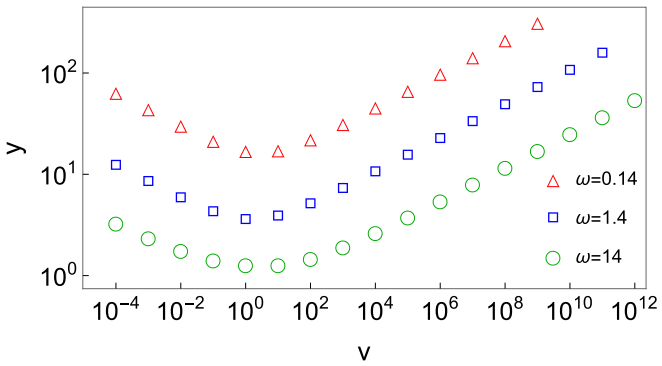

FIG. 9. Bipolarness y of a tactoid as a function of the dimensionless volume v in the presence of an electric field for different values of the anchoring strength, indicated by the symbols. Dimensionless field strength $\Gamma = 100$ and bend constant $\kappa = 10$.

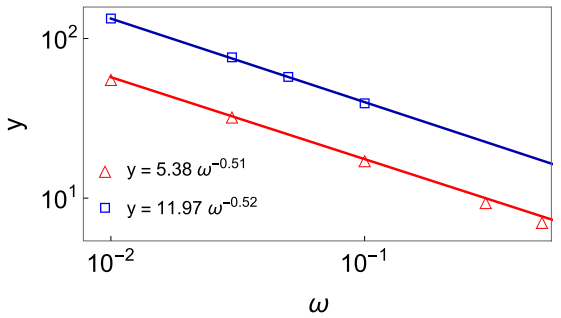

FIG. 11. Bipolarness y of a tactoid as a function of anchoring strength ($\omega < 1$) for small and large droplets, with dimensionless volumes $v = 10^{-2}$ and 10^6. The dimensionless electric field strength is fixed at $\Gamma = 10$ and the dimensionless bend constant at $\kappa = 0$. Indicated are also the scaling relations $y \sim \omega^{-0.51}$ and $y \sim \omega^{-0.52}$. See also the main text.

regimes for $\omega < 1$ for which the droplets are approximately spherical, and $\omega > 1$ for which they are elongated, are also illustrated in the figure. Four different scaling exponents, which agree rather well with the predictions from scaling theory, are shown in the figure.

How the value of the bend elastic constant κ impacts the dependence of the bipolarness y and the anchoring strength ω is highlighted in Fig. 12 for a large and small value of κ. For the range of anchoring strengths shown, a small tactoid volume of $v = 10^{-4}$ and a field strength of $\Gamma = 10^2$, we find scaling exponents of -0.43 and -0.90 for the small and large values of dimensionless bend constants κ, which have to be compared with the scaling predictions of $-\frac{5}{12} \simeq -0.42$ and $-\frac{11}{12} \simeq -0.92$. Again, we find quite good agreement between our numerical work and the scaling theory. (See also Table II.)

Having exhaustively verified the theoretical scaling predictions for the degree of bipolarness of the tactoids, we now proceed to investigate how their aspect ratio depends on the volume and how it responds to the presence of an electric field. It is well known that, in the absence of an electric field, the aspect ratio of a nematic tactoid decreases with increasing droplet size. This happens to be so not only in bulk, but also if the tactoids deposited on a partially wetting surface [5,12,39].

Indeed, from the scaling theory we expect that for $v > v_-$, the aspect ratio x should scale as $v^{-1/5}$ at least if $\kappa \ll \omega$ and $\omega \to \infty$ [12,28,29]. For finite $\omega = 14$ the decay of the aspect ratio with volume is even a weaker function of the volume, as Fig. 13 shows for the field-free case $\Gamma = 0$.

Notice that for the dimensionless bend constant of $\kappa = 10$, the predicted critical magnetic field strength of $\Gamma_* = \frac{1}{11} \simeq 0.09$ coincides with the smallest nonzero value of Γ taken in our numerical calculations. This means that our results of Fig. 13 should show conditions characterized by an absence of an intermediate regime with spherical tactoids, excluding the case $\Gamma = 0$. See also the phase diagram of Fig. 4. The predicted crossover volume $v_* \sim \Gamma^{-5/4}$ from a decreasing aspect ratio to an increasing aspect ratio varies five orders of magnitude for the range of field strengths shown in the figure, in agreement with our numerical results presented in the figure.

What Fig. 13 also shows is that for increasingly large fields, the drop in aspect ratio becomes small mirroring the prediction of our scaling theory. This happens for $\Gamma > \Gamma_c \sim \omega^2/(1 + \kappa/\omega) \simeq 100$ for our choice of parameters, when the drop in aspect ratio in fact disappears. This value is consistent with our numerical findings. In that case, the director field is

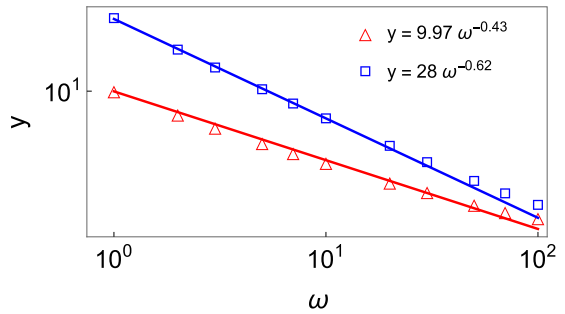

FIG. 10. Bipolarness y of a tactoid as a function of an anchoring strength $\omega > 1$ for small and large droplets, with dimensionless volumes $v = 10^{-2}$ and 10^6. The dimensionless electric field strength is fixed at $\Gamma = 10$ and the dimensionless bend constant at $\kappa = 0$. Indicated are also the scaling relations $y \sim \omega^{-0.43}$ for the small volume and $y \sim \omega^{-0.62}$ for the large volume. See also the main text.

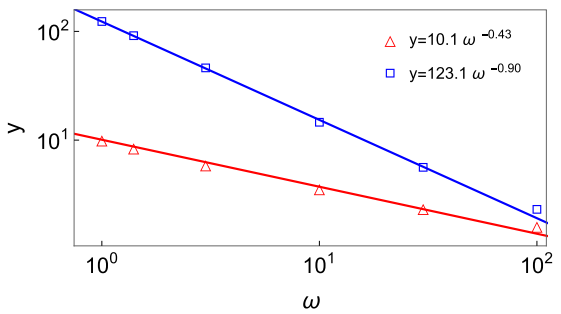

FIG. 12. Bipolarness y as a function of anchoring strength ω for two different dimensionless bend constants of $\kappa = 0.1$ and 10^3. The dimensionless volume is set at a value $v = 10^{-4}$. Also indicated are the scaling exponent of -0.43 for the small value of the bend constant and of -0.90 for the large value of the constant. See also the main text.

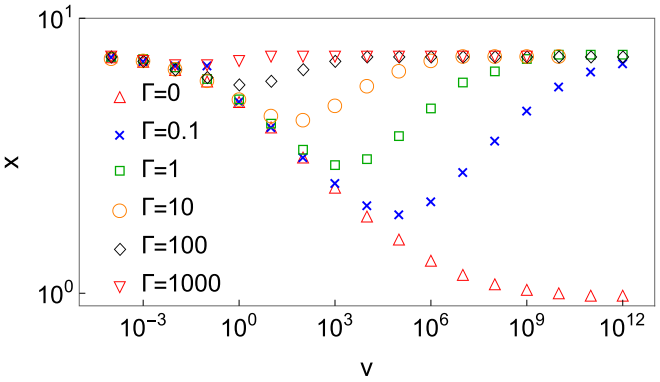

FIG. 13. The aspect ratio x of a tactoid as a function of the dimensionless volume v for different (dimensionless) electric field strengths Γ indicated by the symbols. The anchoring strength is set at $\omega = 14$ and the dimensionless bend constant at $\kappa = 10$.

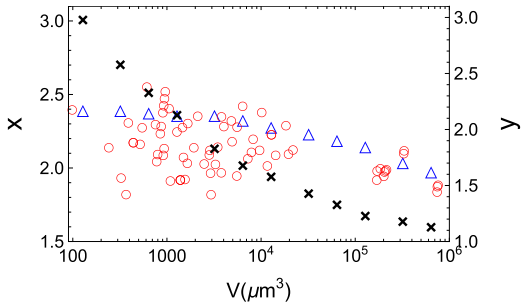

FIG. 14. Aspect ratio x and bipolarness y of the director field as a function of volume of a droplet in the absence of the electric field with $\Gamma = 0$. Left vertical axis shows us the aspect ratio (we use blue triangles for the aspect ratio) and the right vertical axis shows us bipolarness (cross signs for bipolarness) and the red circles represent the experimental data of [39]. The best fits we obtain by eye are for the parameter values $\kappa = 20$, $\omega = 1.3$, and $(K_{11} - K_{24})/\sigma = 4$ μm. Notice that the largest tactoids are bipolar because $y \to 1$ and the smallest ones quasibipolar with $y \approx 3$.

for all intents and purposes uniform irrespective of the volume of the nematic droplet. This means that in our model, there is an upper limit for the aspect ratio, namely $2\sqrt{\omega}$.

All of this implies that for our choice of director field geometry, an externally applied electric (or magnetic) field *cannot* elongate tactoids beyond their maximum aspect ratio that under the field-free conditions happens for sufficiently small droplets. This, clearly, goes against the grain of the experimental observations of Metselaar *et al.* of tactoids in electric fields [39], and those of Kaznacheev and collaborators in magnetic fields [26]. As we argue in the next section, this must mean that either (i) the director field does not conform to a bispherical geometry in an external alignment field; (ii) the tactoids are in a restricted equilibrium characterized by a bipolarness that is fixed to the value of the field-free initial state; or (iii) the various elastic and surface constants do depend on the strength of the field.

V. DISCUSSION AND CONCLUSIONS

In this paper, we present a model in which the director field and shape of a nematic tactoid can adjust themselves both in order to optimize the interfacial, elastic, and Coulomb energy in the presence of an externally applied orienting field. We restrict the shape of the tactoid to that of the family of circle sections of revolution, and the director field to that of the family of fields that can be described by bispherical geometries [61,62]. We find that the known "phase" diagram of nematic tactoids becomes more complex in the presence of an electric field [28–30].

In the absence of such an alignment field there are three regimes, separating elongated tactoids with a uniform director field if they are sufficiently small from roundish bipolar ones if very large, with an intermediate size range where the drops are quasibipolar and somewhat elongated. In the presence of an alignment field, we have identified up to five regimes depending on the strength of the anchoring of the director to the interface. A schematic of the new phase diagram is given in Fig. 4.

Close comparison of theoretical predictions based on this model and experimental observations on tactoids of carbon nanotubes in chlorosulfonic acid by Jamali *et al.* have shown that, in the absence of an electric orienting field, there is a very good agreement between the theory and experiments [5]. The predicted gradual crossover from elongated to more or less spherical shapes, and from uniform to bipolar director fields, is confirmed experimentally, not only for tactoids in bulk solution, but also for sessile tactoids, i.e., tactoids on surfaces [12]. Curve fits provide access to information on the surface energies and bend constants [5,12,27,29,63–67].

For instance, if we curve fit the theory to the experimental data of Metselaar *et al.* on tactoids formed in dispersions of chitin fibers in water in the absence of an electric field, we obtain a reasonably good agreement if we set $\omega = 1.6$, $\kappa = 20$, and $(K_{11} - K_{24})/\sigma = 4$ μm. See Fig. 14, where the aspect ratio x is plotted against the actual volume of the droplets. Also shown in the figure is the predicted bipolarness y of the tactoids, which vary between 3 and just over 1 over that range of droplet volumes. It suggests that the tactoids of chitin in water are either bipolar or quasibipolar, in agreement with experimental observation [39].

Because of the scatter in the data, and since we do not cover the whole range of volumes from nearly uniform to bipolar director fields as was done in the work of Jamali *et al.* [5], we cannot expect these estimates to be highly accurate. Still, if we take them at face value, we find them to differ quite substantially from the ones found by Jamali *et al.* for carbon nanotubes in chlorosulfonic acid, with $\omega = 5.6$, $\kappa = 1.3$, and $(K_{11} - K_{24})/\sigma = 78$ μm [5]. This, however, should not be too surprising, given that both the elastic constants and surface energies depend sensitively on the dimensions of the particles [35,55,57].

Rather unexpectedly, our predictions fail if an external field is applied. In the experiments of Metselaar *et al.*, sufficiently large tactoids elongate up to 10 times their original aspect ratio, which is much more elongated than the droplets in the absence of a field [39]. As we have seen in our model calculations, the presence of very large field strengths does *not* lead to highly elongated shapes but to uniform director fields. As already announced, this might perhaps suggest that the

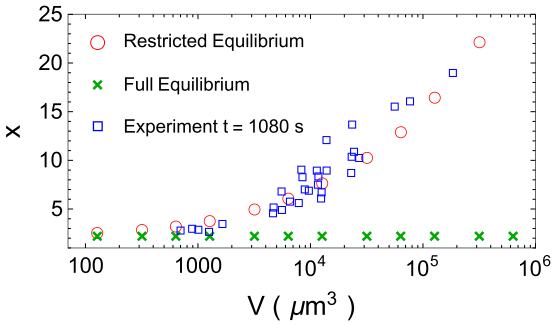

FIG. 15. Aspect ratio x of tactoids as a function of volume V in the presence of an electric field. We compare our numerical results with the experimental data of [39]. The best fit by eye we obtain taking as parameter values $\Gamma = 500$, $\omega = 1.3$, $\kappa = 20$, and $(K_{11} - K_{24})/\sigma = 4\ \mu$m.

bipolarness of the tactoids cannot respond sufficiently swiftly to the switching on of the external field. Before discussing the accuracy of this presumption, we first investigate its consequences assuming that it is true.

The procedure that we pursue is as follows. First we calculate the bipolarness y of the director field for the field-free case with $\Gamma = 0$. Next, in the presence of an orienting field, so for $\Gamma > 0$, we use this value of the bipolarness and optimize the free energy only with respect to the aspect ratio x. Following this procedure, we do find a strong elongation of the droplets as Fig. 15 shows, where we compare the prediction of the full equilibrium and this *restricted-equilibrium* model with the dynamical data of Metselaar *et al.* for tactoids of chitin in water. Shown is the aspect ratio of the droplets as a function of their volumes for a single electric-field strength. For the largest droplets, the full relaxation takes more than the maximum of 1100 s, so the tactoids have not fully equilibrated yet (see Fig. 15 of [39]).

It seems that within a restricted-equilibrium calculation, agreement with the experimental data is indeed rather good, even if they do not yet represent fully relaxed tactoids. The data confirm our expectation that the electric field only has an impact on the shape of the tactoids if they are sufficiently large. How large depends on the strength of the electric field. This is shown in Fig. 16, where we show predictions of our restricted-equilibrium model for the aspect ratio x of nematic droplets as a function of the dimensionless volume v for

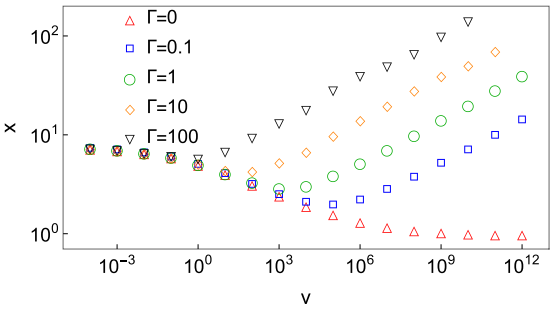

FIG. 16. Aspect ratio x of a tactoid as a function of the dimensionless volume v for different electric-field strengths Γ according to the restricted equilibrium model. See the main text. Anchoring strength $\omega = 14$ and bend elastic constant $\kappa = 10$.

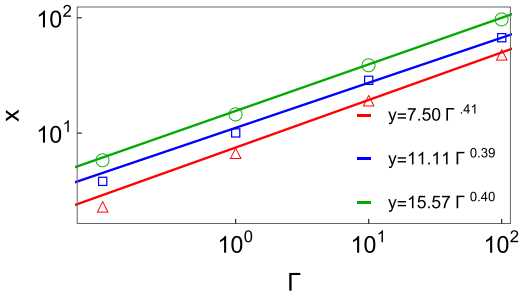

FIG. 17. Aspect ratio x of a tactoid as a function of the electric field Γ according to the restricted-equilibrium model. Anchoring strength $\omega = 14$ and dimensionless bend constant $\kappa = 10$. Different symbols show different volumes: triangles $v = 10^7$, squares $v = 10^8$, and circles $v = 10^9$. Indicated are also the scaling exponents, which are close to 0.4 for the three tactoid volumes.

different dimensionless field strengths Γ. According to the scaling theory of Sec. III, we should expect an $x \sim \Gamma^{3/7} v^{1/7}$ for a fully bipolar director field corresponding to sufficiently large droplets. The slopes of the various curves shown in Fig. 16 agree with this. Figure 17 shows that the scaling with the electric field strength Γ for different tactoid volumes v also agrees with the scaling prediction of $\frac{3}{7} \approx 0.43$.

All of this of course begs the question why our full equilibrium model, in which the tactoids choose their optimal aspect ratio and director field in response to the external field, does not agree with the experimental observations. Above we have presumed that the bipolarness of the tactoids cannot respond swiftly to the switching on of an electric field, at least less swiftly than the aspect ratio can respond. In that case, a restricted equilibrium picture applies, which would be valid for intermediate times. This implies that after an initial increase in aspect ratio, this aspect ratio should decrease again for (potentially) much later times. This has not yet been investigated but would be an interesting avenue of future experimental research.

While this may seem a somewhat far-fetched explanation to align theory and experiment, it does tie in with the observations of Jamali *et al.*, who collected data on hundreds of tactoids of carbon nanotubes in chlorosulfonic acid [5]. Even after 15 days of equilibration, the scatter in the observed aspect ratio remains appreciable and cannot be explained by thermal fluctuations. Indeed, the experiments of Metselaar *et al.* also point at long relaxation times: the largest droplets do not seem completely equilibrated even after 7000 s. On the other hand, the lattice Boltzmann simulations presented in the work of Metselaar *et al.* [39], which do mirror the large elongation of the tactoids in an external field, point at a relatively swift relaxation of the director field after the external field is switched on.

In the simulations, the director field seems to keep the almost perfect planar alignment to the interface of the tactoid with the surrounding isotropic fluid, while in the bulk of the tactoid the director field seems to become homogeneous [41]. This suggests a different kind of relaxation of the director field in response to the alignment field than the one we presumed in our work, which conserves the geometry of director field. This kind of director field is in our view surprising, as it involves

a strong deformation with a small radius of curvature that is very costly in elastic free energy. This is why, generally, it is believed that wall defects in nematics spread out very quickly [34]. (See, however, Tromp *et al.* [68].) We emphasize that, in general, the interplay of the defective points (disclinations) and curvature is not trivial. The complexity arises from solving the elasticity equations in three dimensions (3D) in the presence of defects [69,70].

In fact, a simple scaling theory supports this view in the context of tactoids. Let us for simplicity take a spherical tactoid of radius R. A locally deformed director field that preserves perfect planar anchoring would give a free energy of the form $F \simeq \sigma R^2 + KR^2\xi^{-1} + \gamma R^2\xi$. Here, K is some combination of the bend and splay elastic constants, $\xi \leqslant R$ is the width of the deformed director field that we equate to its radius of curvature, and $\gamma = \epsilon_a E^2$ is the Coulomb energy per unit volume. If we optimize ξ, we get $\xi = K_{11}^{1/2}\gamma^{-1/2} \leqslant R$ for $\gamma \geqslant K_{11}R^{-2}$. For $\gamma \leqslant KR^{-2}$, we have $\xi = R$.

Hence, we obtain $F \simeq \sigma R^2 + KR + \gamma R^3$ for $\gamma \leqslant KR^{-2}$ and $F \simeq \sigma R^2 + \gamma^{1/2} + K^{1/2}R^2$ for $\gamma \geqslant KR^{-2}$. For a smooth director field in the limit of large field strengths, we have $F \simeq \sigma R^2 + \sigma\omega R^2$ because the director field is then approximately uniform. This shows that for $\gamma \geqslant \omega\sigma/R$ the uniform director field has a lower free energy than the locally deformed one. Of course, we cannot exclude the possibility that for $KR^{-2} < \gamma < \omega\sigma/R$ a locally deformed director field wins out albeit that this might also be accompanied by an imperfect anchoring.

In conclusion, we should perhaps not exclude the possibility that the lattice Boltzmann simulations, which are coarse grained and characterized by rather large interfacial widths even on the scale of the width of the droplets, allow for larger deformations in the interfacial region than a continuum theory would. Because of this, we feel that additional and more comprehensive simulation studies would be useful to perform in order to settle this issue [71].

Finally, we cannot exclude the possibility that the external field has a sizable impact on both the interfacial tension, the anchoring, and on the elastic constants because they all depend on the degree of orientation order of the particles [35,48,49]. Indeed, all of them depend on the degree of alignment of the particles, where we note that the isotropic phase becomes paranematic in the presence of an external field [52,72,73]. This implies that the interfacial tension between the nematic droplets and the host phase should decrease with increasing field strength. In fact, it should disappear altogether at some critical field strength. The study presented in this paper shows that these issues can only be resolved with more detailed experimental investigation of the impact of external fields on the properties of isotropic and nematic phases of rodlike colloidal particles.

ACKNOWLEDGMENTS

This work was supported by the National Science Foundation through Grant No. DMR-1719550.

[1] J. van Duijneveldt and D. Frenkel, Computer simulation study of free energy barriers in crystal nucleation, J. Chem. Phys. **96**, 4655 (1992).

[2] R. van Roij, The isotropic and nematic liquid crystal phase of colloidal rods, Eur. J. Phys. **26**, S57 (2005).

[3] M. P. Lettinga, K. Kang, A. Imhof, D. Derks, and J. K. G. Dhont, Kinetic pathways of the nematic–isotropic phase transition as studied by confocal microscopy on rod-like viruses, J. Phys.: Condens. Matter **17**, S3609 (2005).

[4] M. P. Lettinga, K. Kang, P. Holmqvist, A. Imhof, D. Derks, and J. K. G. Dhont, Nematic-isotropic spinodal decomposition kinetics of rodlike viruses, Phys. Rev. E **73**, 011412 (2006).

[5] V. Jamali, N. Behabtu, B. Senyuk, J. A. Lee, I. I. Smalyukh, P. van der Schoot, and M. Pasquali, Experimental realization of crossover in shape and director field of nematic tactoids, Phys. Rev. E **91**, 042507 (2015).

[6] S. Fraden, A. Hurd, R. Meyer, M. Cahoon, and D. Caspar, Magnetic-field-induced alignment and instabilities in ordered colloids of tobacco mosaic virus, J. Phys. Colloq. **46**, C3 (1985).

[7] H. Zöcher, Über freiwillige Strukturbildung in Solen. (Eine neue Art anisotrop flüssiger Medien.), Z. Anorg. Allg. Chem. **147**, 91 (1925).

[8] F. C. Bawden, Liquid crystalline substances from virus-infected plants, Nature (London) **138**, 1051 (1936).

[9] K. Coper and H. Freundlich, The formation of tactoids in iron oxide sols, Trans. Faraday Soc. **33**, 348 (1937).

[10] C. Robinson, Liquid-crystalline structures in solutions of a polypeptide, Trans. Faraday Soc. **52**, 571 (1956).

[11] N. Puech, E. Grelet, P. Poulin, C. Blanc, and P. van der Schoot, Nematic droplets in aqueous dispersions of carbon nanotubes, Phys. Rev. E **82**, 020702(R) (2010).

[12] V. Jamali, E. G. Biggers, P. van der Schoot, and M. Pasquali, Line tension of twist-free carbon nanotube lyotropic liquid crystal microdroplets on solid surfaces, Langmuir **33**, 9115 (2017).

[13] Z. Dogic, Surface Freezing and a Two-Step Pathway of the Isotropic-Smectic Phase Transition in Colloidal Rods, Phys. Rev. Lett. **91**, 165701 (2003).

[14] A. Modlińska, A. M. Alsayed, and T. Gibaud, Condensation and dissolution of nematic droplets in dispersions of colloidal rods with thermosensitive depletants, Sci. Rep. **5**, 18432 (2015).

[15] P. W. Oakes, J. Viamontes, and J. X. Tang, Growth of tactoidal droplets during the first-order isotropic to nematic phase transition of F-actin, Phys. Rev. E **75**, 061902 (2007).

[16] K. L. Weirich, S. Banerjee, K. Dasbiswas, T. A. Witten, S. Vaikuntanathan, and M. L. Gardel, Liquid behavior of cross-linked actin bundles, Proc. Natl. Acad. Sci. USA **114**, 2131 (2017).

[17] K. L. Weirich, K. Dasbiswas, T. A. Witten, S. Vaikuntanathan, and M. L. Gardel, Self-organizing motors divide active liquid droplets, Proc. Natl. Acad. Sci. USA **116**, 11125 (2019).

[18] Y.-K. Kim, S. V. Shiyanovskii, and O. D. Lavrentovich, Morphogenesis of defects and tactoids during isotropic–nematic phase transition in self-assembled lyotropic chromonic liquid crystals, J. Phys.: Condens. Matter **25**, 404202 (2013).

[19] D. Marenduzzo, A. Flammini, A. Trovato, J. R. Banavar, and A. Maritan, Physics of thick polymers, J. Polym. Sci., Part B: Polym. Phys. **43**, 650 (2005).

[20] H.-S. Kitzerow, Polymer-dispersed liquid crystals from the nematic curvilinear aligned phase to ferroelectric films, Liq. Cryst. **16**, 1 (1994).

[21] J. H. Park, J. Noh, C. Schütz, G. Salazar-Alvarez, G. Scalia, L. Bergström, and J. P. F. Lagerwall, Macroscopic control of helix orientation in films dried from cholesteric liquid-crystalline cellulose nanocrystal suspensions, ChemPhysChem **15**, 1477 (2014).

[22] P.-X. Wang, W. Y. Hamad, and M. J. MacLachlan, Structure and transformation of tactoids in cellulose nanocrystal suspensions, Nat. Commun. **7**, 11515 (2016).

[23] J.-F. Revol, H. Bradford, J. Giasson, R. Marchessault, and D. Gray, Helicoidal self-ordering of cellulose microfibrils in aqueous suspension, Int. J. Biol. Macromol. **14**, 170 (1992).

[24] S. Chandrasekhar, Surface tension of liquid crystals, Mol. Cryst. Liq. Cryst. **2**, 71 (1966).

[25] O. D. Lavrentovich, Topological defects in dispersed liquid crystals, or words and worlds around liquid crystal drops, Liq. Cryst. **24**, 117 (1998).

[26] A. V. Kaznacheev, M. M. Bogdanov, and S. A. Taraskin, The nature of prolate shape of tactoids in lyotropic inorganic liquid crystals, J. Exp. Theor. Phys. **95**, 57 (2002).

[27] A. Kaznacheev, M. Bogdanov, and A. Sonin, The influence of anchoring energy on the prolate shape of tactoids in lyotropic inorganic liquid crystals, J. Exp. Theor. Phys. **97**, 1159 (2003).

[28] P. Prinsen and P. van der Schoot, Shape and director-field transformation of tactoids, Phys. Rev. E **68**, 021701 (2003).

[29] P. Prinsen and P. van der Schoot, Continuous director-field transformation of nematic tactoids, Eur. Phys. J. E **13**, 35 (2004).

[30] P. Prinsen and P. van der Schoot, Parity breaking in nematic tactoids, J. Phys.: Condens. Matter **16**, 8835 (2004).

[31] R. M. W. van Bijnen, R. H. J. Otten, and P. van der Schoot, Texture and shape of two-dimensional domains of nematic liquid crystals, Phys. Rev. E **86**, 051703 (2012).

[32] R. H. J. Otten and P. van der Schoot, Deformable homeotropic nematic droplets in a magnetic field, J. Chem. Phys. **137**, 154901 (2012).

[33] J. C. Everts, M. T. J. J. M. Punter, S. Samin, P. van der Schoot, and R. van Roij, A landau-de gennes theory for hard colloidal rods: Defects and tactoids, J. Chem. Phys. **144**, 194901 (2016).

[34] P. G. De Gennes and J. Prost, *The Physics of Liquid Crystals* (Oxford University Press, Oxford, 1993).

[35] P. van der Schoot, Remarks on the interfacial tension in colloidal systems, J. Phys. Chem. B **103**, 8804 (1999).

[36] D. Marenduzzo, E. Orlandini, and J. M. Yeomans, Permeative Flows in Cholesteric Liquid Crystals, Phys. Rev. Lett. **92**, 188301 (2004).

[37] R. D. Williams, Two transitions in tangentially anchored nematic droplets, J. Phys. A: Math. Gen. **19**, 3211 (1986).

[38] D. Vanzo, M. Ricci, R. Berardi, and C. Zannoni, Shape, chirality and internal order of freely suspended nematic nanodroplets, Soft Matter **8**, 11790 (2012).

[39] L. Metselaar, I. Dozov, K. Antonova, E. Belamie, P. Davidson, J. M. Yeomans, and A. Doostmohammadi, Electric-field-induced shape transition of nematic tactoids, Phys. Rev. E **96**, 022706 (2017).

[40] Tactoids can also be stretched by the effect an elongational flow field, as was recently shown by H. Almohammadi, M. Bagnani, and R. Mezzenga, Flow-induced order–order transitions in amyloid fibril liquid crystalline tactoids, Nat. Commun. **11**, 5416 (2020).

[41] L. Metselaar (private communication).

[42] E. G. Virga, *Variational Theories for Liquid Crystals* (CRC Press, Boca Raton, FL, 1994).

[43] A. Rapini and M. Papoular, Distorsion d'une lamelle nématique sous champ magnétique conditions d'ancrage aux parois, J. Phys. Colloq. **30**, C4 (1969).

[44] Z. Y. Chen and J. Noolandi, Numerical solution of the onsager problem for an isotropic-nematic interface, Phys. Rev. A **45**, 2389 (1992).

[45] L. D. Landau and E. M. Lifshitz, *Course of Theoretical Physics* (Elsevier, Amsterdam, 2013).

[46] M. Doi and S. F. Edwards, *The Theory of Polymer Dynamics* (Oxford University Press, Oxford, 1988).

[47] B. Lev, V. Nazarenko, A. Nych, and P. Tomchuk, Deformation and instability of nematic drops in an external electric field, J. Exp. Theor. Phys. Lett. **71**, 262 (2000).

[48] J. Straley, The gas of long rods as a model for lyotropic liquid crystals, Mol. Cryst. Liq. Cryst. **22**, 333 (1973).

[49] T. Odijk, Elastic constants of nematic solutions of rod-like and semi-flexible polymers, Liq. Cryst. **1**, 553 (1986).

[50] G. J. Vroege and H. N. Lekkerkerker, Phase transitions in lyotropic colloidal and polymer liquid crystals, Rep. Prog. Phys. **55**, 1241 (1992).

[51] H. Wensink and G. Vroege, Isotropic–nematic phase behavior of length-polydisperse hard rods, J. Chem. Phys. **119**, 6868 (2003).

[52] A. Khokhlov and A. Semenov, Influence of external field on the liquid-crystalline ordering in the solutions of stiff-chain macromolecules, Macromolecules **15**, 1272 (1982).

[53] A. Semenov, Interaction of point defects in a nematic liquid, Europhys. Lett. **46**, 631 (1999).

[54] See Supplemental Material at http://link.aps.org/supplemental/10.1103/PhysRevE.103.062703 for the shape of bipolar coordinate that we use to find bispherical coordinate.

[55] W. Chen and D. G. Gray, Interfacial tension between isotropic and anisotropic phases of a suspension of rodlike particles, Langmuir **18**, 633 (2002).

[56] É. Generalova, A. Kaznacheev, and A. Sonin, Effect of magnetic field on lyotropic nematic in the vanadium pentoxide (V_2O_5)-water system, Crystallogr. Rep. **46**, 111 (2001).

[57] T. Sato and A. Teramoto, On the frank elastic constants of lyotropic polymer liquid crystals, Macromolecules **29**, 4107 (1996).

[58] C. F. Dietrich, P. J. Collings, T. Sottmann, P. Rudquist, and F. Giesselmann, Extremely small twist elastic constants in lyotropic nematic liquid crystals, Proc. Natl. Acad. Sci. USA **117**, 27238 (2020).

[59] A. Verhoeff, R. Otten, P. van der Schoot, and H. Lekkerkerker, Magnetic field effects on tactoids of plate-like colloids, J. Chem. Phys. **134**, 044904 (2011).

[60] A. Verhoeff, I. Bakelaar, R. Otten, P. van der Schoot, and H. Lekkerkerker, Tactoids of plate-like particles: Size, shape, and director field, Langmuir **27**, 116 (2011).

[61] P. Lucht, Bipolar coordinates and the two-cylinder capacitor, Rimrock Digital Technology, Salt Lake City, Utah **84103** (2015).

[62] https://en.wikipedia.org/wiki/bipolar_coordinates.

[63] M. Bagnani, P. Azzari, S. Assenza, and R. Mezzenga, Six-fold director field configuration in amyloid nematic and cholesteric phases, Sci. Rep. **9**, 12654 (2019).

[64] P.-X. Wang and M. J. MacLachlan, Liquid crystalline tactoids: Ordered structure, defective coalescence and evolution in confined geometries, Philos. Trans. R. Soc. A **376**, 20170042 (2018).

[65] G. Nyström and R. Mezzenga, Liquid crystalline filamentous biological colloids: Analogies and differences, Curr. Opin. Colloid Interface Sci. **38**, 30 (2018).

[66] R. K. Bharadwaj, T. J. Bunning, and B. Farmer, A mesoscale modelling study of nematic liquid crystals confined to ellipsoidal domains, Liq. Cryst. **27**, 591 (2000).

[67] A. DeBenedictis and T. J. Atherton, Shape minimisation problems in liquid crystals, Liq. Cryst. **43**, 2352 (2016).

[68] R. H. Tromp and P. van der Schoot, Quench-induced nematic textures of wormlike micelles, Phys. Rev. E **53**, 689 (1996).

[69] S. Li, P. Roy, A. Travesset, and R. Zandi, Why large icosahedral viruses need scaffolding proteins, Proc. Natl. Acad. Sci. USA **115**, 10971 (2018).

[70] R. Zandi, B. Dragnea, A. Travesset, and R. Podgornik, On virus growth and form, Phys. Rep. **847**, 1 (2020).

[71] A. Kuhnhold and P. van der Schoot (unpublished).

[72] S.-D. Lee, Comment on effects of elongational flow on the isotropic–nematic phase transition in rod-like systems, J. Chem. Phys. **86**, 6567 (1987).

[73] S. Varga, G. Jackson, and I. Szalai, External field induced paranematic-nematic phase transitions in rod-like systems, Mol. Phys. **93**, 377 (1998).